Supplement of Atmos. Chem. Phys., 15, 5457–5469, 2015
http://www.atmos-chem-phys.net/15/5457/2015/
doi:10.5194/acp-15-5457-2015-supplement
© Author(s) 2015. CC Attribution 3.0 License.

Atmospheric Chemistry and Physics
Open Access

Supplement of

Free amino acids in Antarctic aerosol: potential markers for the evolution and fate of marine aerosol

E. Barbaro et al.

Correspondence to: E. Barbaro (barbaro@unive.it)

The copyright of individual parts of the supplement might differ from the CC-BY 3.0 licence.

Reagents and standard solutions

Ultra grade methanol (MeOH) was purchased from Romil LTD (Cambridge, UK), while Ultrapure water (18.2 MΩ, 0.01 TOC) was produced using a Purelab Ultra System (Elga, High Wycombe,UK). Formic acid (≥98%) eluent additive for HPLC system was obtained from Fluka (Sigma Aldrich®, Buchs, Switzerland) and hydrochloric acid (HCl) 37% ACS was supplied by Carlo Erba.

Each amino acid standard solution (D and L-alanine (D-/L-Ala), D and L-arginine (D-/L-Arg), D and L – asparagine (D-/L-Asn), D and L-aspartic acid (D-/L-Asp), D and L -glutamic acid (D-/L-Glu), glycine (Gly), D and L hydroxy proline (D-/L-Hyp), D and L –histidine (D-/L-Hys), D and L –isoleucine (D-/L-Ile), D and L – leucine (D-/L-Leu),D and L –methionine (D-/L-Met), D/L methionine sulfone ($MetSO_2$), L ornithine (L-Orn), D and L –phenylalanine (D-/L-Phe), L-proline (L-Pro), D and L –serine (D-/L-Ser), D and L –threonine (D-/L-Thr), D and L –tyrosine (D-/L-Tyr), D and L tryptophan (D-/L-Trp), and D and L –valine(D-/L-Val)) was prepared from a solid standard (purity ≥98%), and diluted in HCl 0.1M. The solid standards were purchased from Sigma Aldrich®. Isotopically-labeled 13C amino acids (L-[$^{13}C_3$] alanine (Ala*), L-[$^{13}C_4$] aspartic acid (Asp*), L-[$^{13}C_5$] glutamic acid (Glu*), and L-[$^{13}C_6$] arginine (Arg*); purity of 98%) were purchased from Sigma Aldrich while L-[$^{13}C_1$] leucine (Leu*), L-[$^{13}C_1$] phenylalanine (Phe*), L-[$^{13}C_1$] proline (Pro*), and L-[$^{13}C_1$] valine (Val*) (purity ≥98%) were obtained from Cambridge Isotope Laboratories Inc. (Andover, MA).

Table S1. Summary of yield, trueness and reproducibility expressed as a relative standard deviation (RSD%) for circular quartz fiber filters. For each amino acid, the internal standard (IS) used for the quantification, the amount of blank filter and the relative method detection limit (MDL)is reported.

	IS	Yield %	RSD %	Error %	RSD %	Blank (ng abs)	MDL (ng abs)
L-Ala	Ala*	51	10	-10	2	151	44
D-Ala	Ala*	62	7	4	3	30	22
L-Arg	Arg*	62	8	-2	9	4	2
D-Arg	Arg*	78	2	0.7	1	4	3.2
L-Asn	Val*	70	9	3	7	10	6
D-Asn	Val*	67	2	-4	9	15	6
L-Asp	Asp*	50	8	-7	6	41	30
D-Asp	Asp*	41	8	2	13	102	50
L-Glu	Glu*	58	7	-6	2	25	6
D-Glu	Glu*	57	9	-1	6	12	8
L-Hyp	Leu*	70	9	7	13	0.2	0.5
D-Hyp	Leu*	74	7	-5	10	1	1.4
L-Hys	Pro*	66	9	6	1	51	16
D-Hys	Pro*	49	7	-8	8	7	10
L-Leu/L-Ile	Leu*	60	5	-7	6	77	32
D-Leu/D-Ile	Leu*	59	5	-13	6	3	5.8
L-Met	Leu*	61	11	-2	8	2	3.2
D-Met	Leu*	65	9	-9	3	8	10
L-Orn	Arg*	43	13	2	14	249	58
L-Phe	Phe*	63	5	-3	4	5	2.8
D-Phe	Phe*	70	4	7	9	6	5.8
L-Pro	Pro*	61	9	-4	3	15	3.8
L-Ser	Phe*	38	17	-2	8	170	138
D-Ser	Phe*	56	15	6	13	98	84
L-Thr	Arg*	65	6	-1	5	10	5
D-Thr	Arg*	72	6	5	6	2	1
L-Trp	Arg*	63	10	5	6	2	5
D-Trp	Arg*	65	10	-0.2	9	1	1.2
L-Tyr	Phe*	66	13	8	10	24	16
D-Tyr	Phe*	67	9	7	10	6	8
L-Val	Val*	61	6	-6	2	57	12
D-Val	Val*	64	10	-5	5	6	3
Gly	Ala*	71	11	3	4	89	50
MetSO2	Leu*	58	8	-5	8	8	14

Table S2. Summary of yield, trueness and reproducibility expressed as relative standard deviation (RSD%) for backup quartz fiber filters (< 0.49 µm). For each amino acid, the internal standard (IS) used for the quantification, the amount of blank filter and the relative method detection limit (MDL) is reported.

	IS	**Yield %**	**RSD %**	**Error %**	**RSD %**	**Blank (ng abs)**	**MDL (ng abs)**
L-Ala	Ala*	51	6	-8	3	226	35
D-Ala	Ala*	61	9	9	7	67	36
L-Arg	Arg*	53	7	-7	2	26	24
D-Arg	Arg*	61	8	8	3	4	3
L-Asn	Val*	55	6	-2	6	45	28
D-Asn	Val*	54	9	6	9	30	28
L-Asp	Asp*	54	6	-2	4	125	35
D-Asp	Asp*	54	9	1	8	51	28
L-Glu	Glu*	54	5	-3	4	99	18
D-Glu	Glu*	50	9	5	7	16	8
L-Hyp	Val*	56	8	3	10	3	4
D-Hyp	Val*	70	8	7	7	4	5
L-Hys	Pro*	57	32	77	15	88	114
D-Hys	Pro*	46	16	-21	10	43	64
L-Leu/L-Ile	Leu*	57	3	-8	9	31	23
D-Leu/D-Ile	Leu*	61	9	-4	2	14	12
L-Met	Leu*	56	9	-9	5	20	19
D-Met	Leu*	51	5	-9	2	11	6
L-Orn	Arg*	42	5	-3	8	275	61
L-Phe	Phe*	60	7	1	6	32	11
D-Phe	Phe*	65	9	4	8	3	2
L-Pro	Pro*	55	5	-4	3	73	42
L-Ser	Phe*	55	7	8	5	597	167
D-Ser	Phe*	42	9	-6	5	422	61
L-Thr	Arg*	63	10	9	1	46	18
D-Thr	Arg*	58	5	7	3	12	9
L-Trp	Phe*	63	9	-5	7	3	4
D-Trp	Phe*	61	9	-1	9	7	10
L-Tyr	Phe*	53	6	2	7	30	34
D-Tyr	Phe*	62	11	7	8	10	8
L-Val	Val*	58	6	-3	2	91	49
D-Val	Val*	50	8	-7	8	5	12
Gly	Ala*	56	6	-1	3	61	37
MetSO2	Leu*	51	9	-9	8	32	23

Table S3. Summary of yield, trueness and reproducibility expressed as relative standard deviation (RSD%) for slotted quartz fiber filters. For each amino acid, the internal standard (IS) used for the quantification the amount of blank filter and the relative method detection limit (MDL) is reported.

	IS	**Yield %**	**RSD %**	**Error %**	**RSD %**	**Blank (ng abs)**	**MDL (ng abs)**
L-Ala	Ala*	72	6	-6	5	57	24
D-Ala	Ala*	*346*	*6*	*450*	*7*	-	-
L-Arg	Arg*	51	7	-9	4	8	4
D-Arg	Arg*	53	3	-1	6	2	1
L-Asn	Val*	32	5	-64	5	0.2	0.2
D-Asn	Val*	190	7	191	9	-	-
L-Asp	Asp*	71	6	1	3	102	51
D-Asp	Asp*	37	26	-3	33	348	107
L-Glu	Glu*	81	2	7	4	0.6	1.1
D-Glu	Glu*	494	10	799	9	-	-
L-Hyp	Leu*	81	4	3	5	0.5	0.2
D-Hyp	Leu	75	5	-8	5	0.5	0.8
L-Hys	Leu*	71	9	1	15	3	3
D-Hys	Asp*	45	8	-5	14	12	9
L-Leu/L-Ile	Leu*	5	65	7	-9	9	7
D-Leu/D-Ile	Leu*	7	72	13	-6	10	8
L-Met	Leu*	61	10	-8	11	5	4
D-Met	Leu*	50	8	-2	8	2.1	0.5
L-Orn	Arg*	50	9	4	8	41	23
L-Phe	Phe*	77	3	-2	3	12	10
D-Phe	Phe*	102	9	56	4	-	-
L-Pro	Pro*	61	7	-8	5	82	56
L-Ser	Phe*	88	10	57	7	-	-
D-Ser	Phe*	-18	-6	-115	-40	-	-
L-Thr	Arg*	57	6	-9	7	19	8
D-Thr	Arg*	64	8	7	4	3	2
L-Trp	Phe*	99	8	59	10	-	-
D-Trp	Phe*	93	6	54	11	-	-
L-Tyr	Arg*	61	4	6	4	12	16
D-Tyr	Arg*	63	7	-13	13	4	7
L-Val	Val*	78	3	-3	3	23	12
D-Val	Val*	174	8	140	7	-	-
Gly	Ala*	36	41	-7	3	36	15
MetSO2	Leu*	66	5	-9	5		4

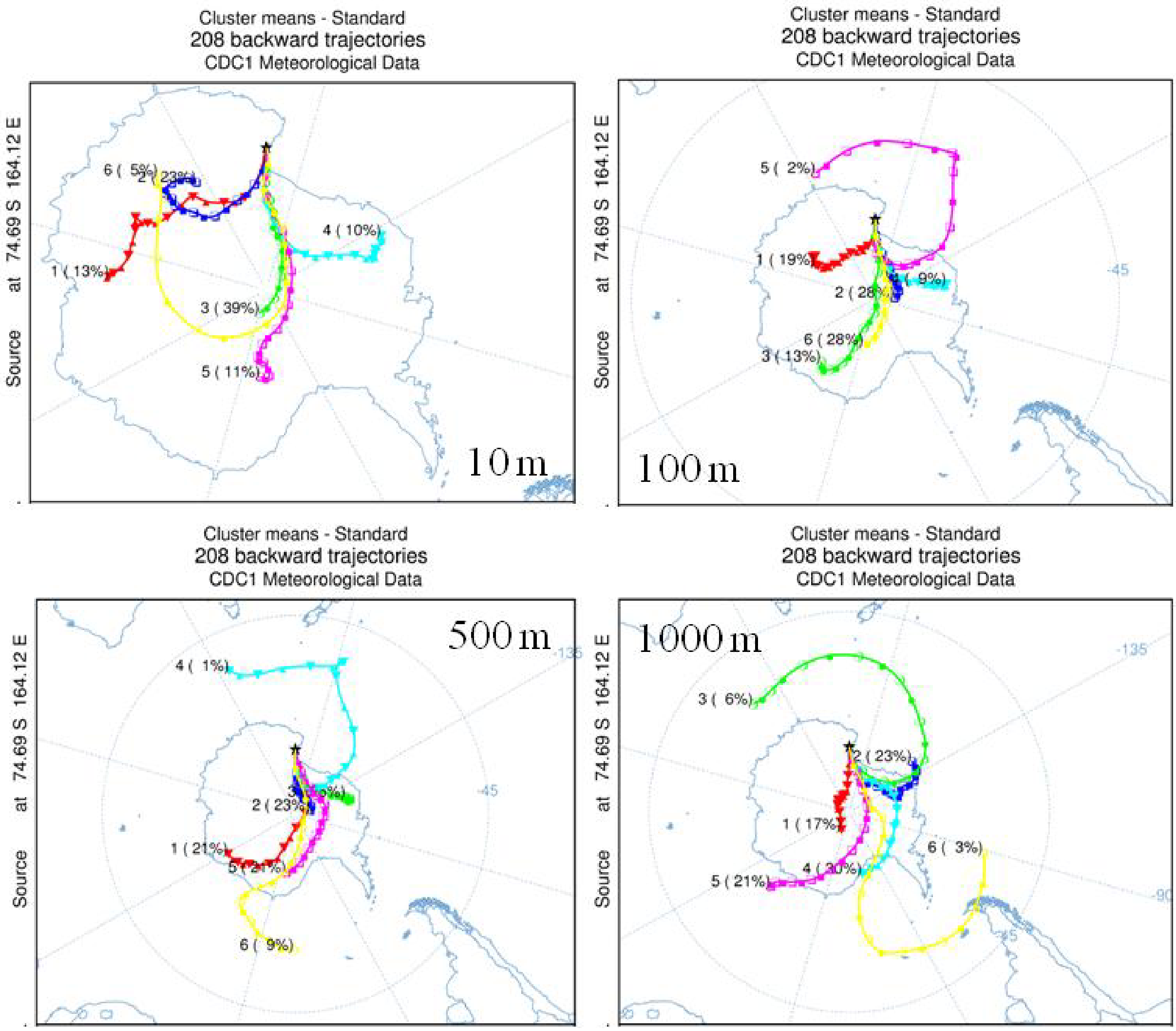

Figure S1. Cluster means backward trajectories analyses at 10 m, 100m, 500m and 1000 m agl at the coastal base “Mario Zucchelli Station” (MZS) during the summer of 2010-2011. Study of the vertical stability of HYSPLIT model. The 208 back trajectories are divided into 6 clusters with the percentage of total number of trajectories that each represents reported in brackets.

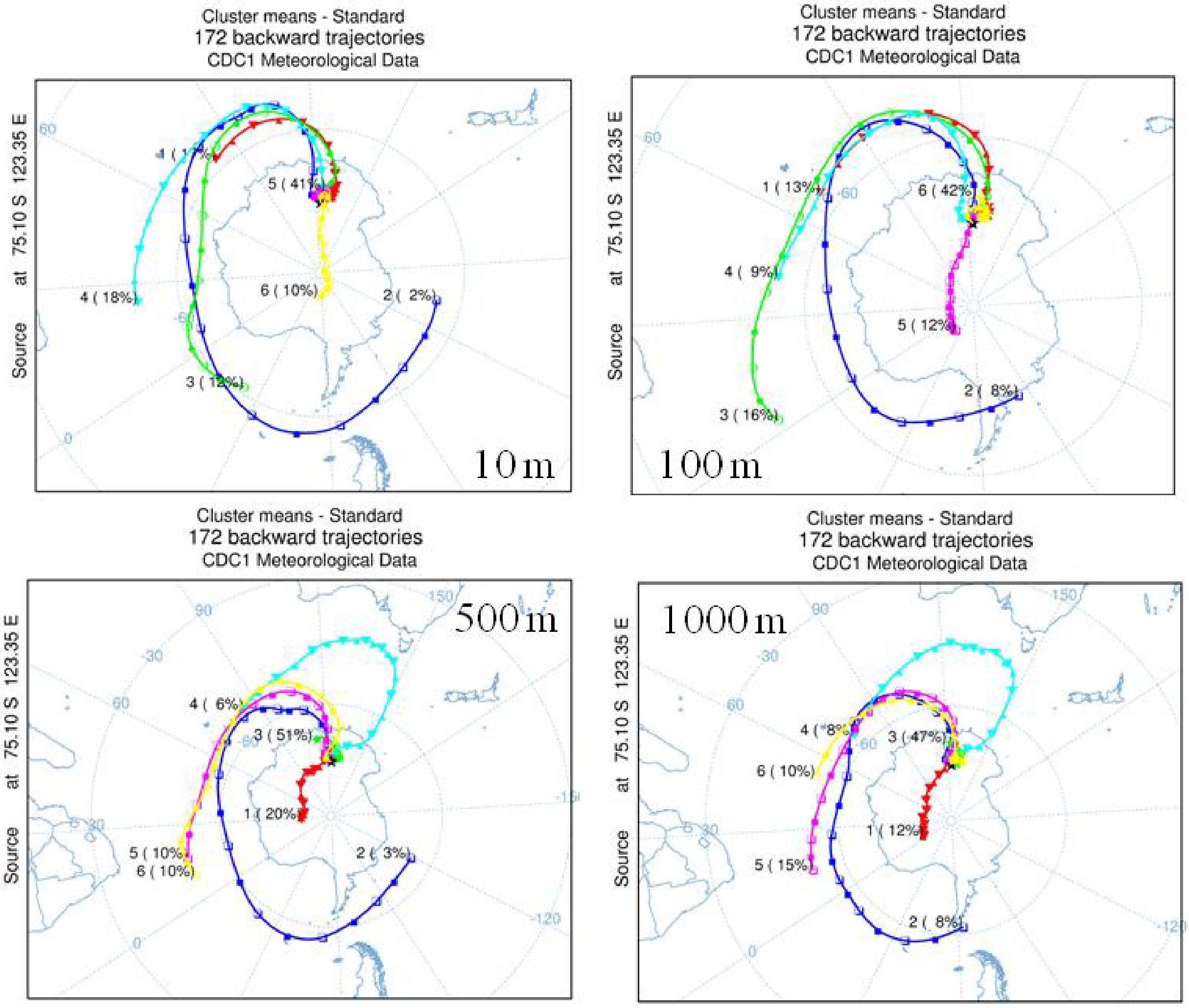

Figure S2. Cluster means backward trajectories analyses at 10 m, 100m, 500m and 1000 m agl at the Italian-French base Dome C (DC) during the summers of 2011-2012. Study of the vertical stability of HYSPLIT model. The 172 back trajectories are divided into 6 clusters with the percentage of total number of trajectories that each represents reported in brackets.

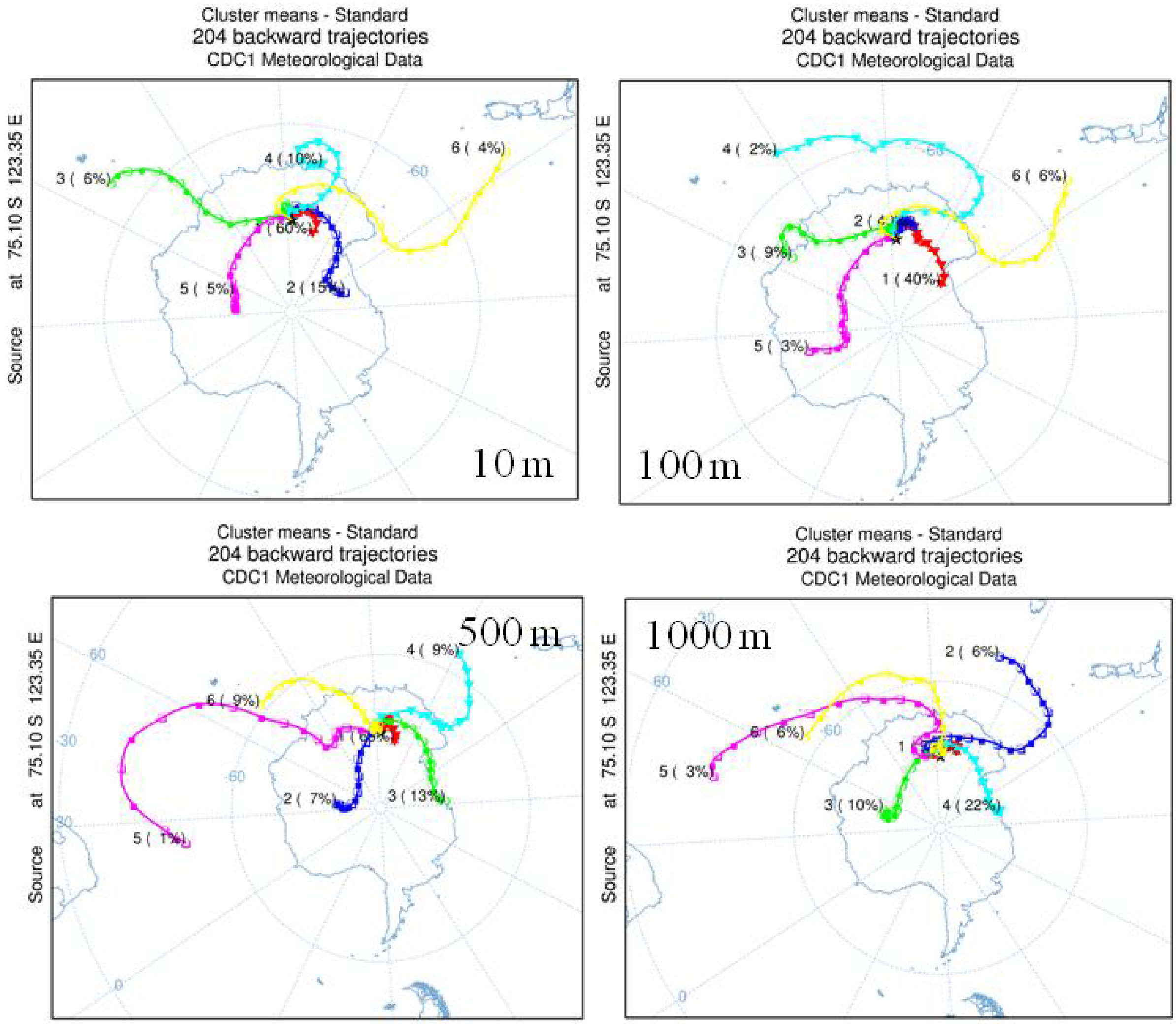

Figure3. Cluster means backward trajectories analyses at 10 m, 100m, 500m and 1000 m agl at the Italian-French base Dome C (DC) during the summers of 2012-2013. Study of the vertical stability of HYSPLIT model. The 204 back trajectories are divided into 6 clusters with the percentage of total number of trajectories that each represents reported in brackets.

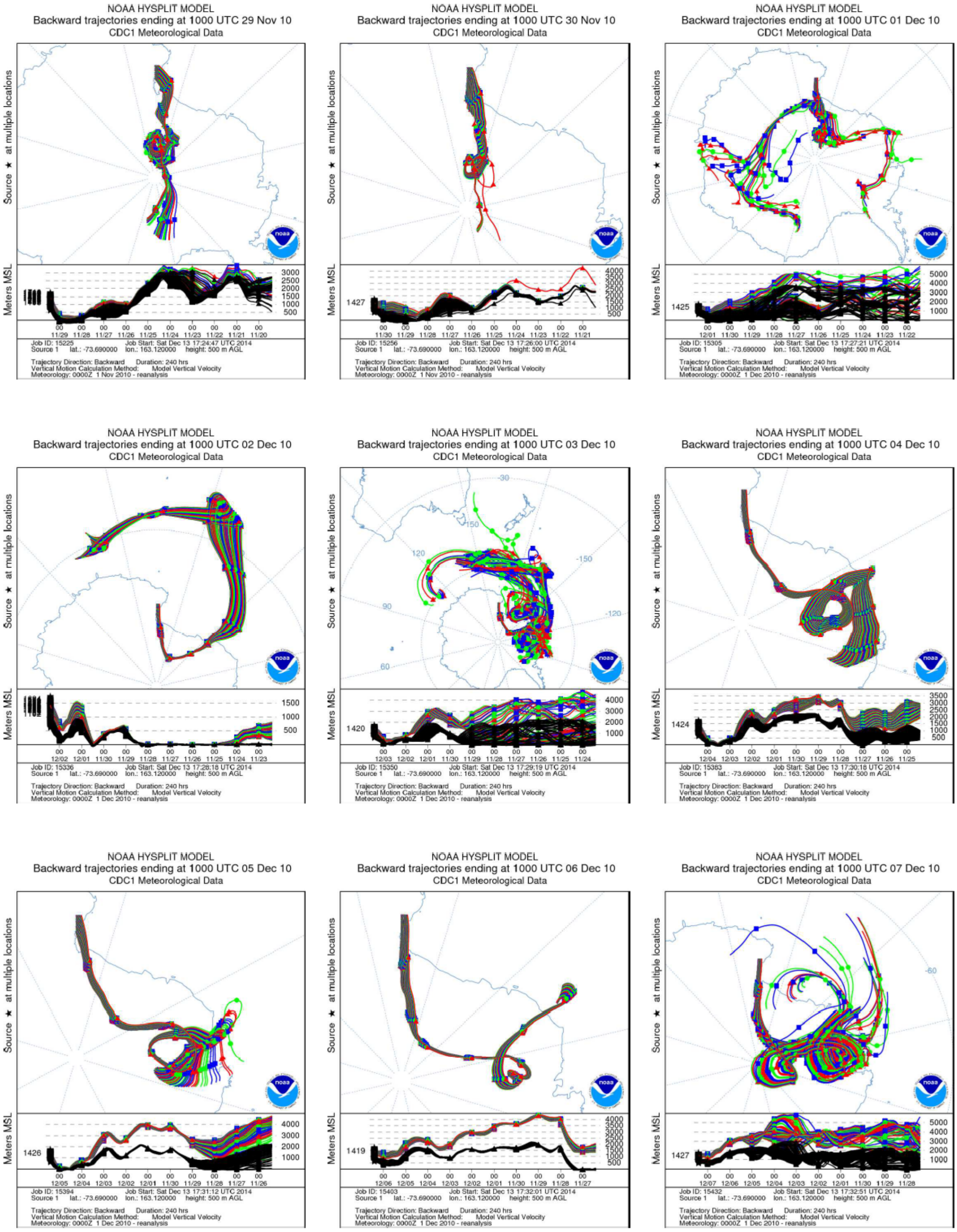

Figure S4. Matrix back-trajectories computed for each 24-h sampling at 500 m agl at the coastal base "Mario Zucchelli Station" (MZS) from the 29th November 2010 to 18th January 2011. Study of the horizontal stability of HYSPLIT model varying the source position of one degree of latitude and longitude from the real coordinates of source.

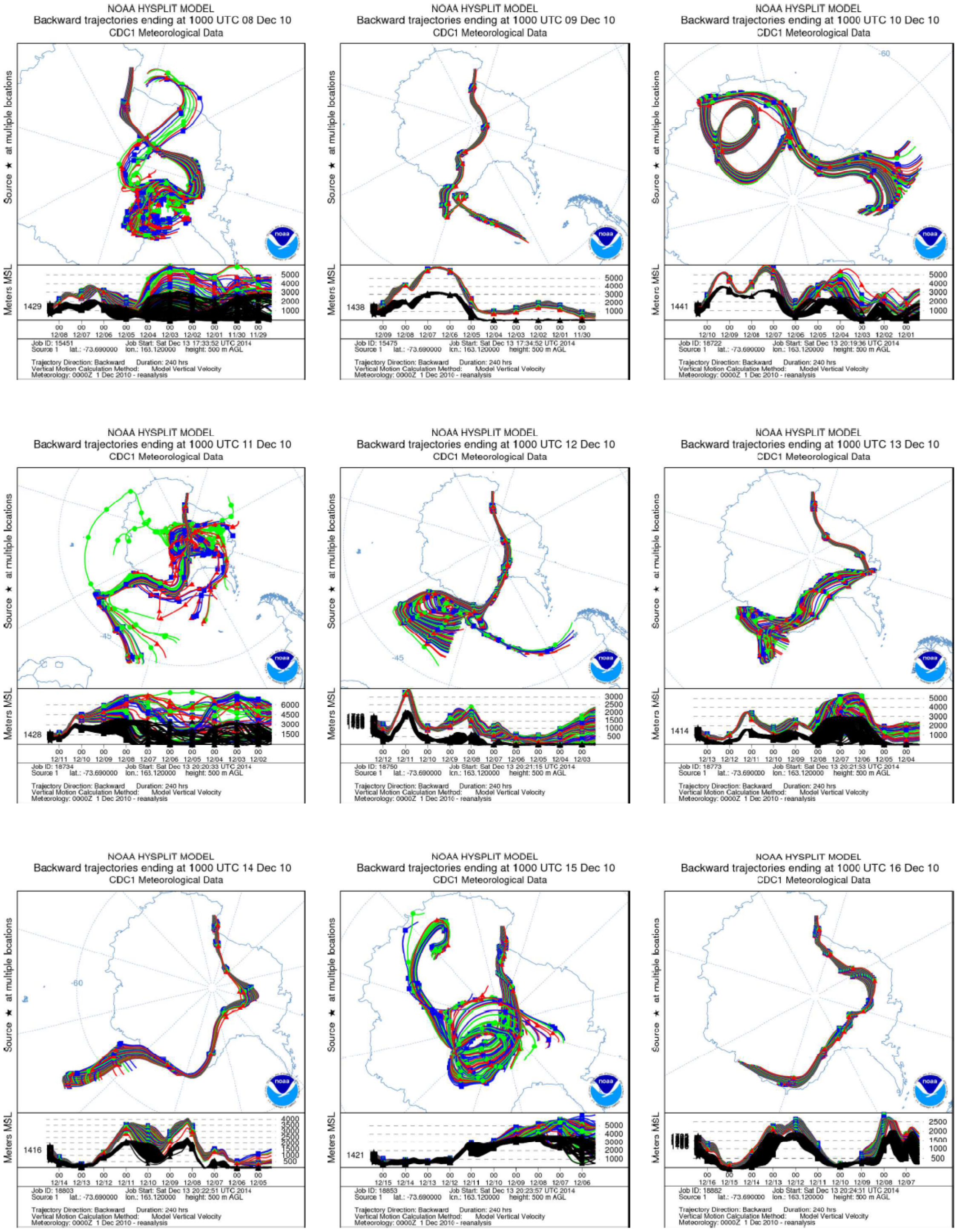

Figure S4. continued

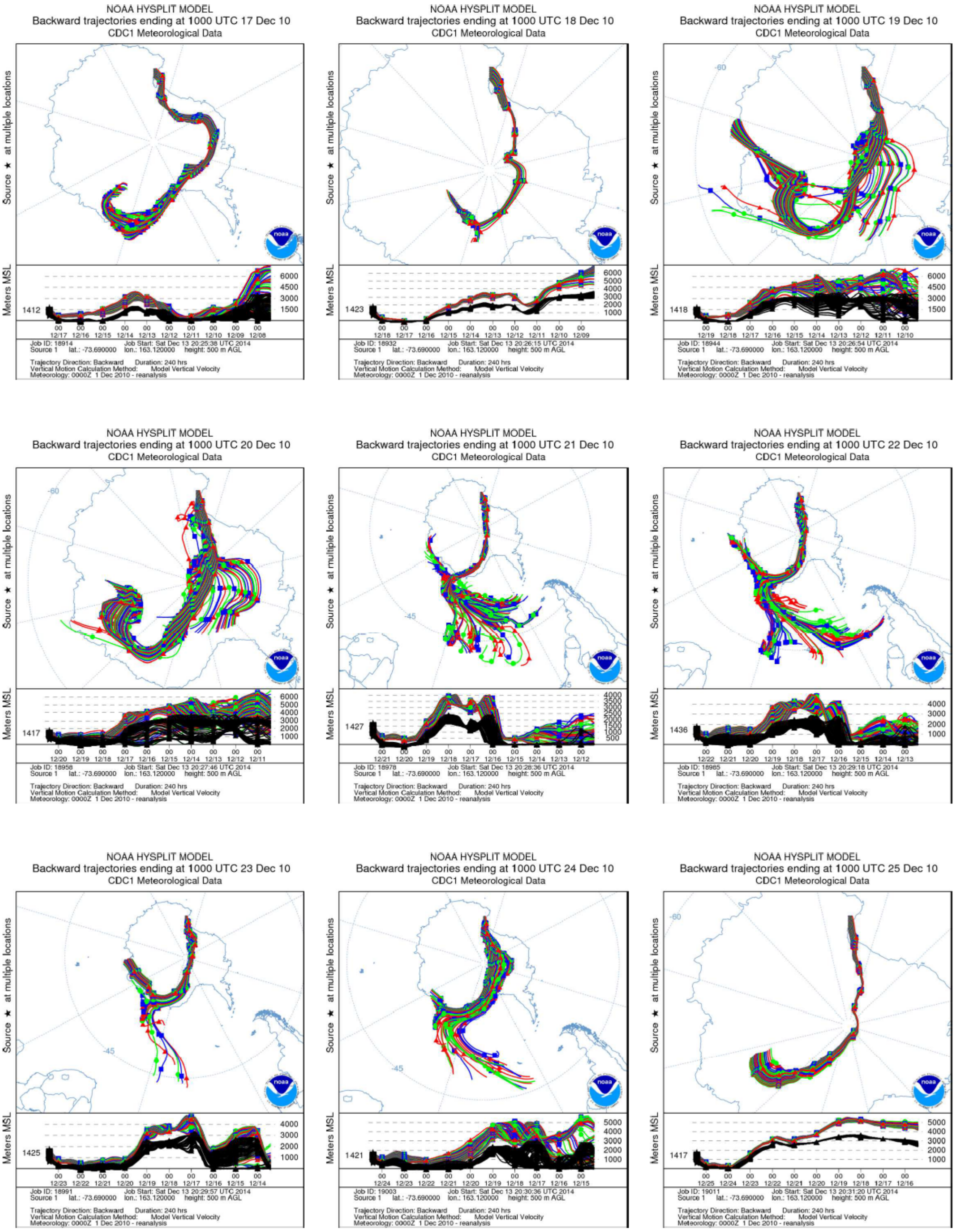

Figure S4. continued

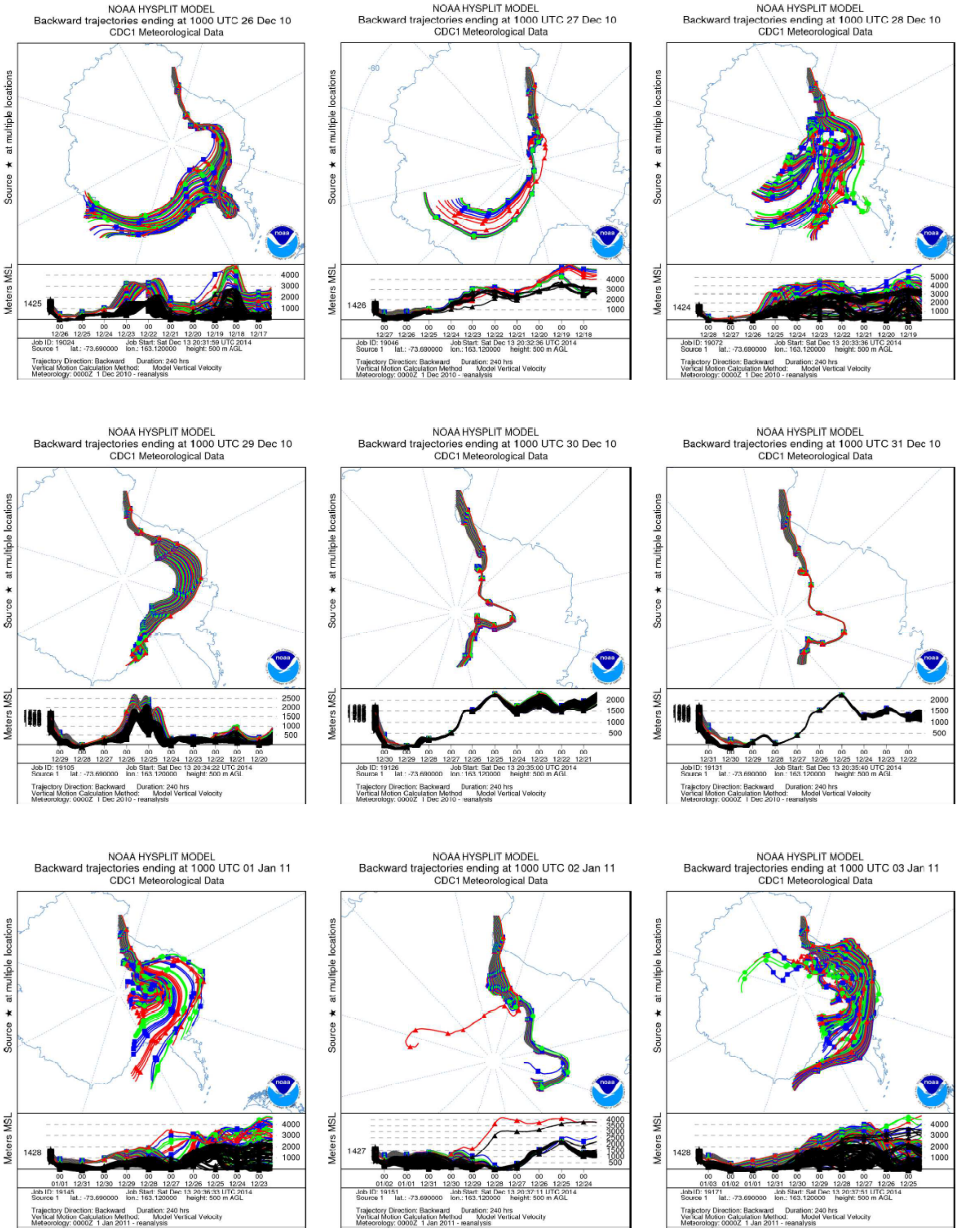

Figure S4. continued

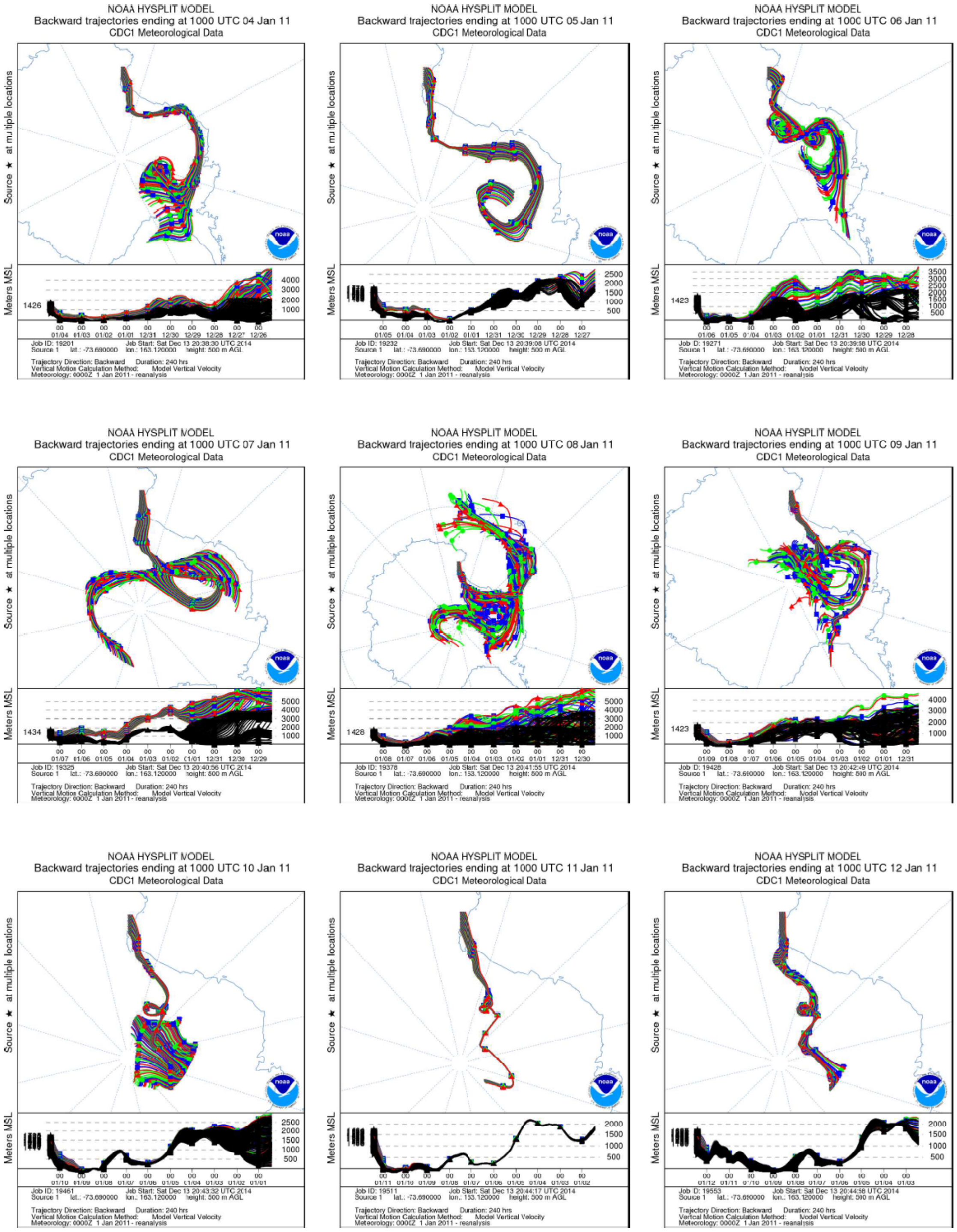

Figure S4. continued

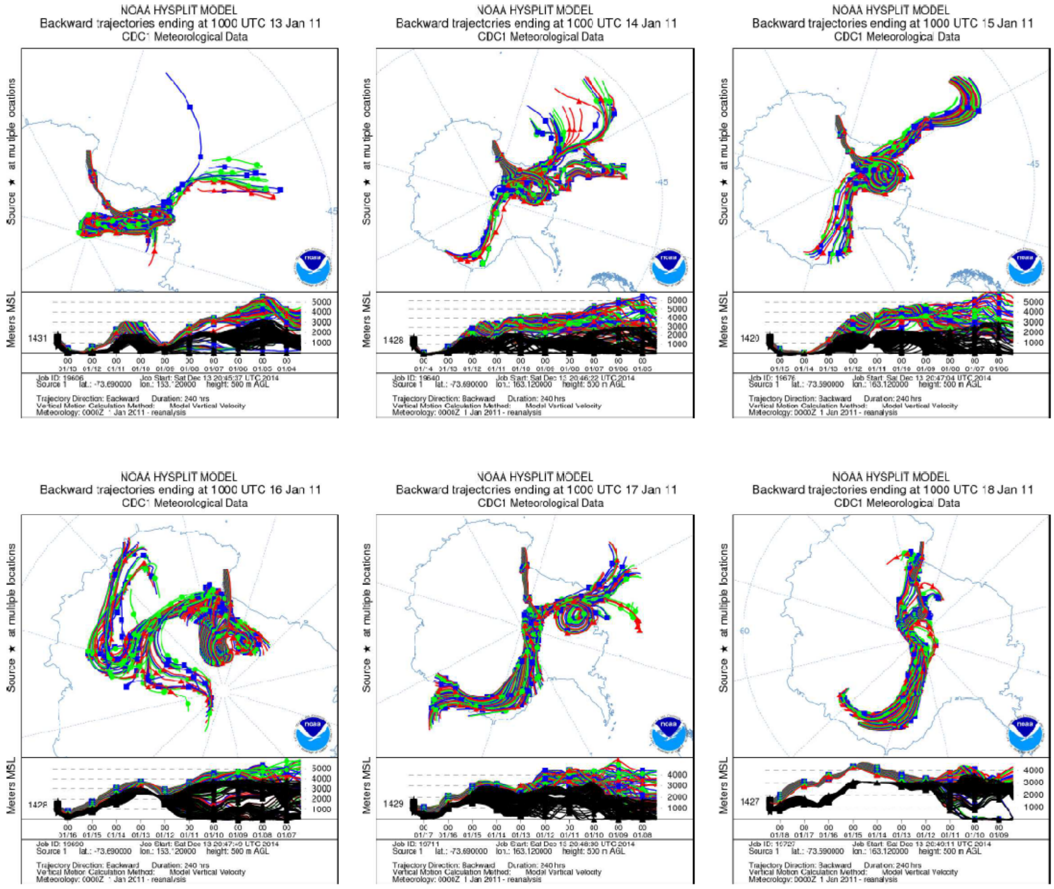

NOAA HYSPLIT MODEL
Backward trajectories ending at 1000 UTC 13 Jan 11
CDC1 Meteorological Data

NOAA HYSPLIT MODEL
Backward trajectories ending at 1000 UTC 14 Jan 11
CDC1 Meteorological Data

NOAA HYSPLIT MODEL
Backward trajectories ending at 1000 UTC 15 Jan 11
CDC1 Meteorological Data

NOAA HYSPLIT MODEL
Backward trajectories ending at 1000 UTC 16 Jan 11
CDC1 Meteorological Data

NOAA HYSPLIT MODEL
Backward trajectories ending at 1000 UTC 17 Jan 11
CDC1 Meteorological Data

NOAA HYSPLIT MODEL
Backward trajectories ending at 1000 UTC 18 Jan 11
CDC1 Meteorological Data

Figure S4. continued

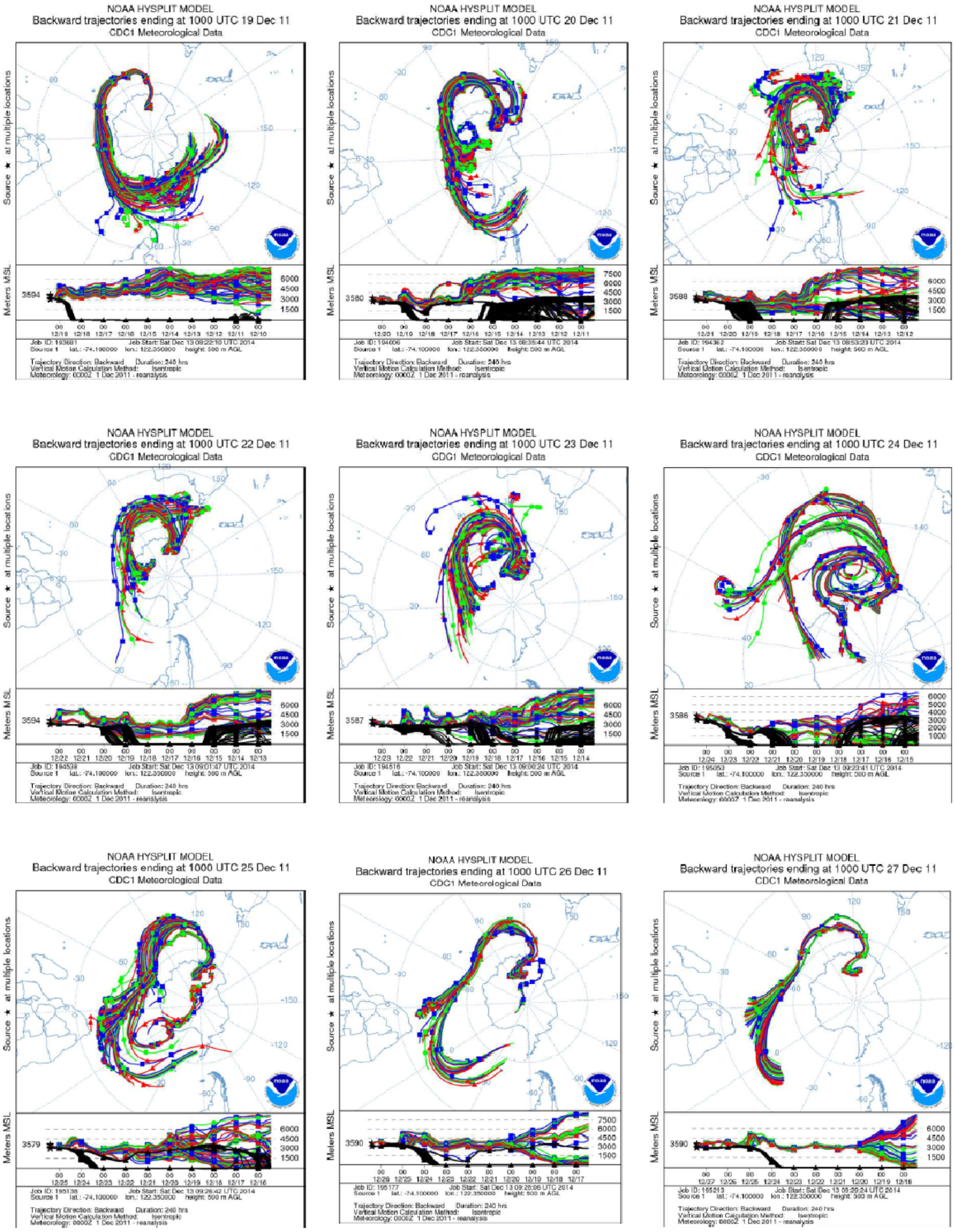

Figure S5. Matrix back-trajectories computed for each 24-h sampling at 500 m agl at the Italian-French base Dome C (DC) 19th December 2011 to 28th January 2012. Study of the horizontal stability of HYSPLIT model varying the source position of one degree of latitude and longitude from the real coordinates of source.

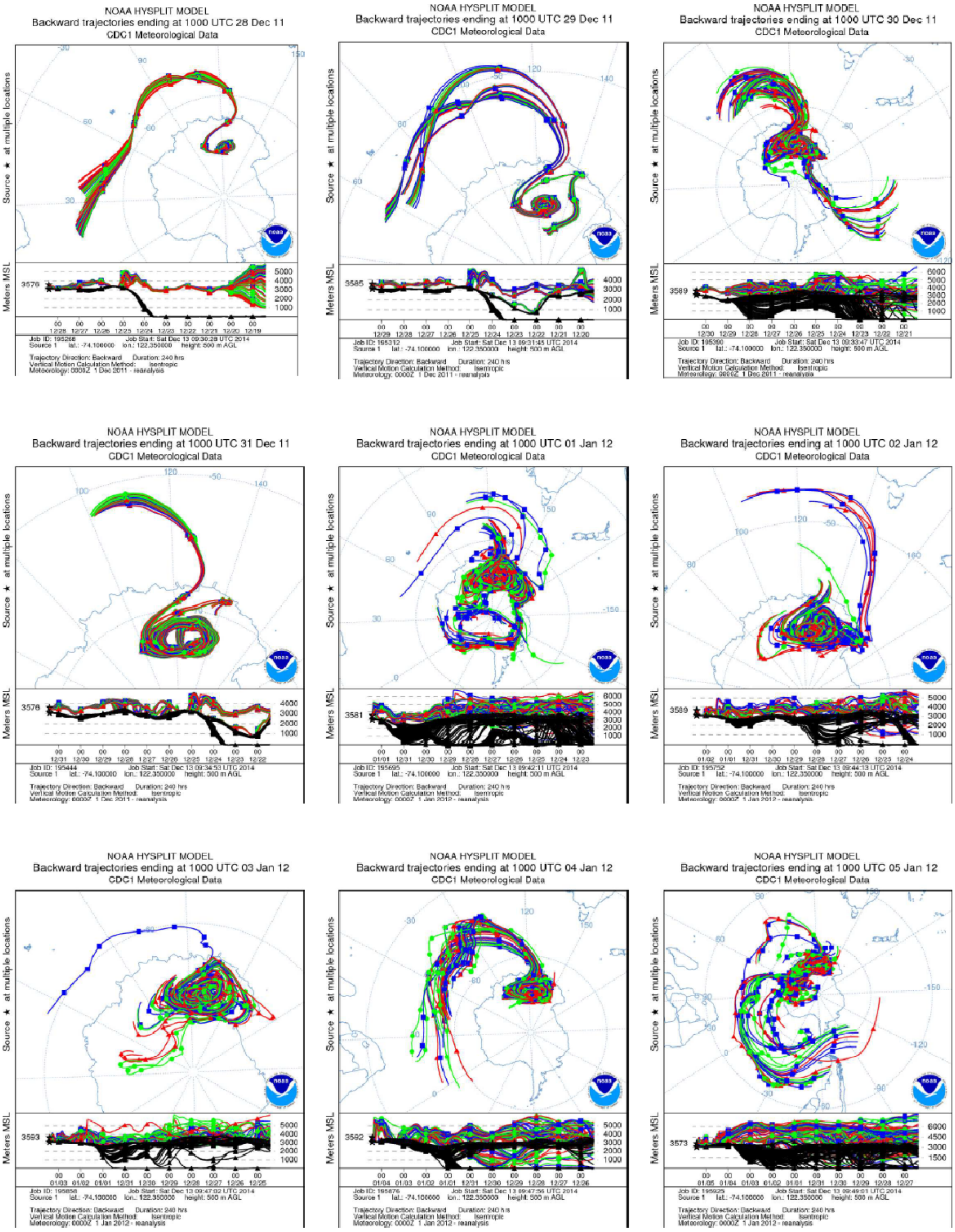

Figure S5. continued

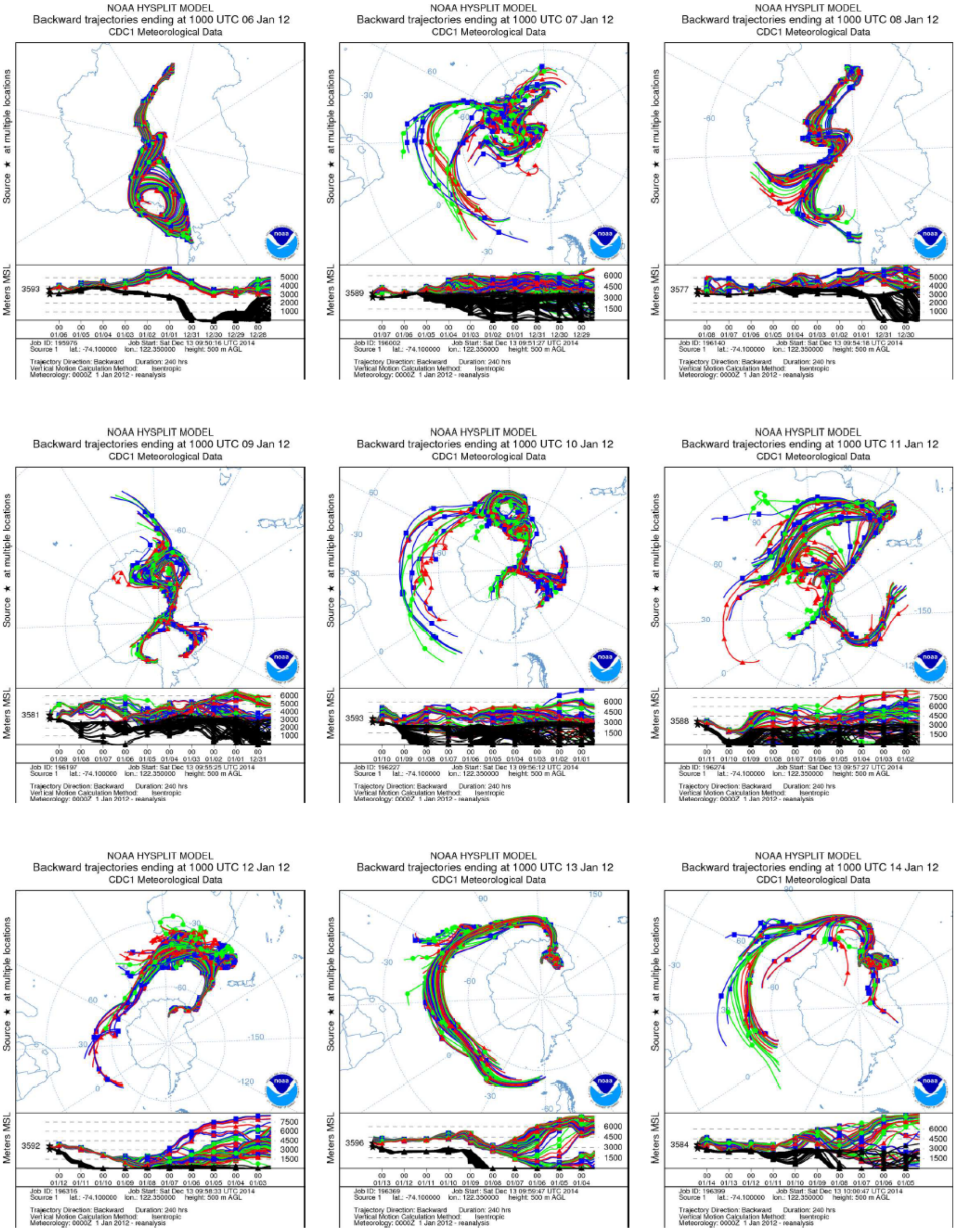

Figure S5. continued

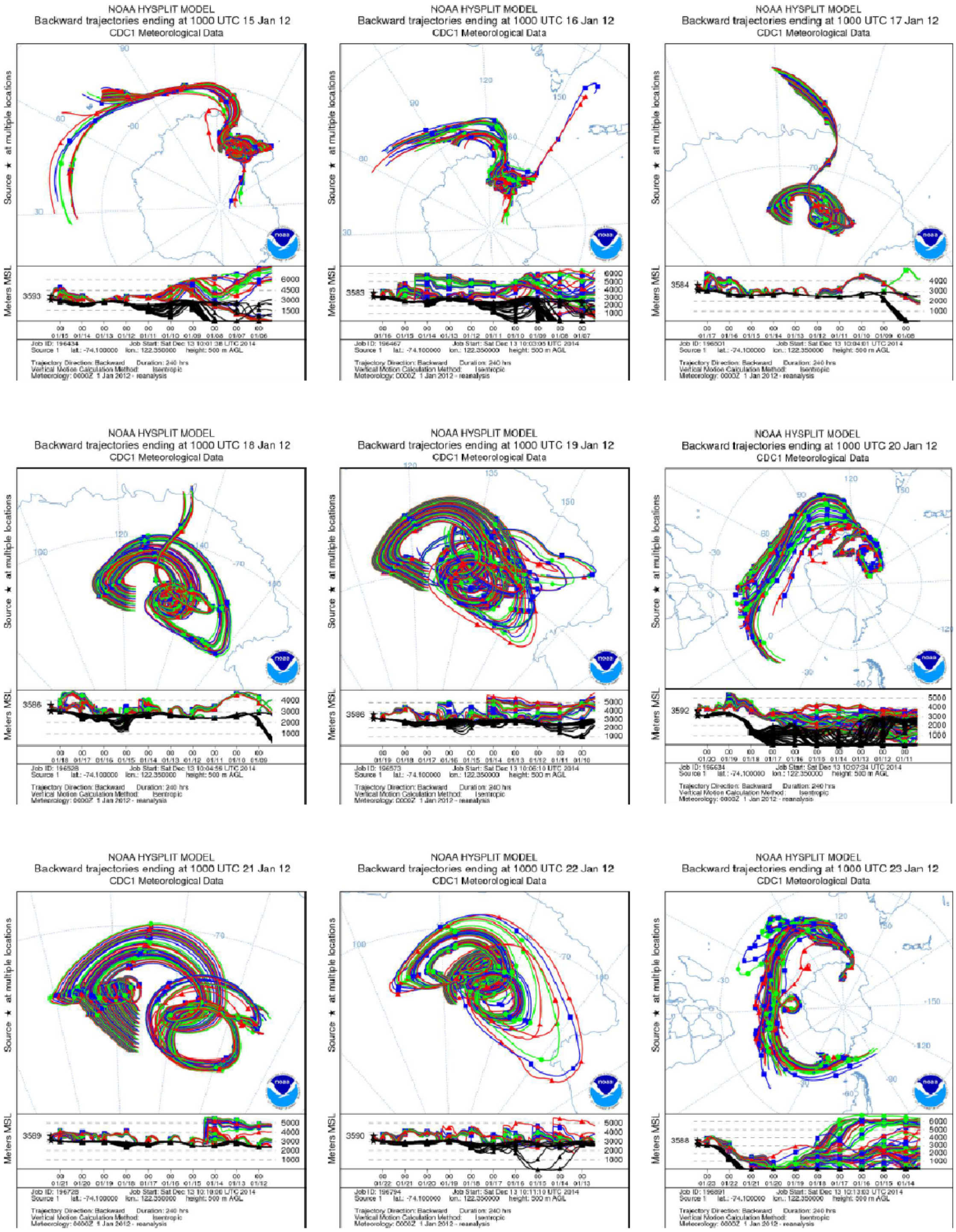

Figure S5. continued

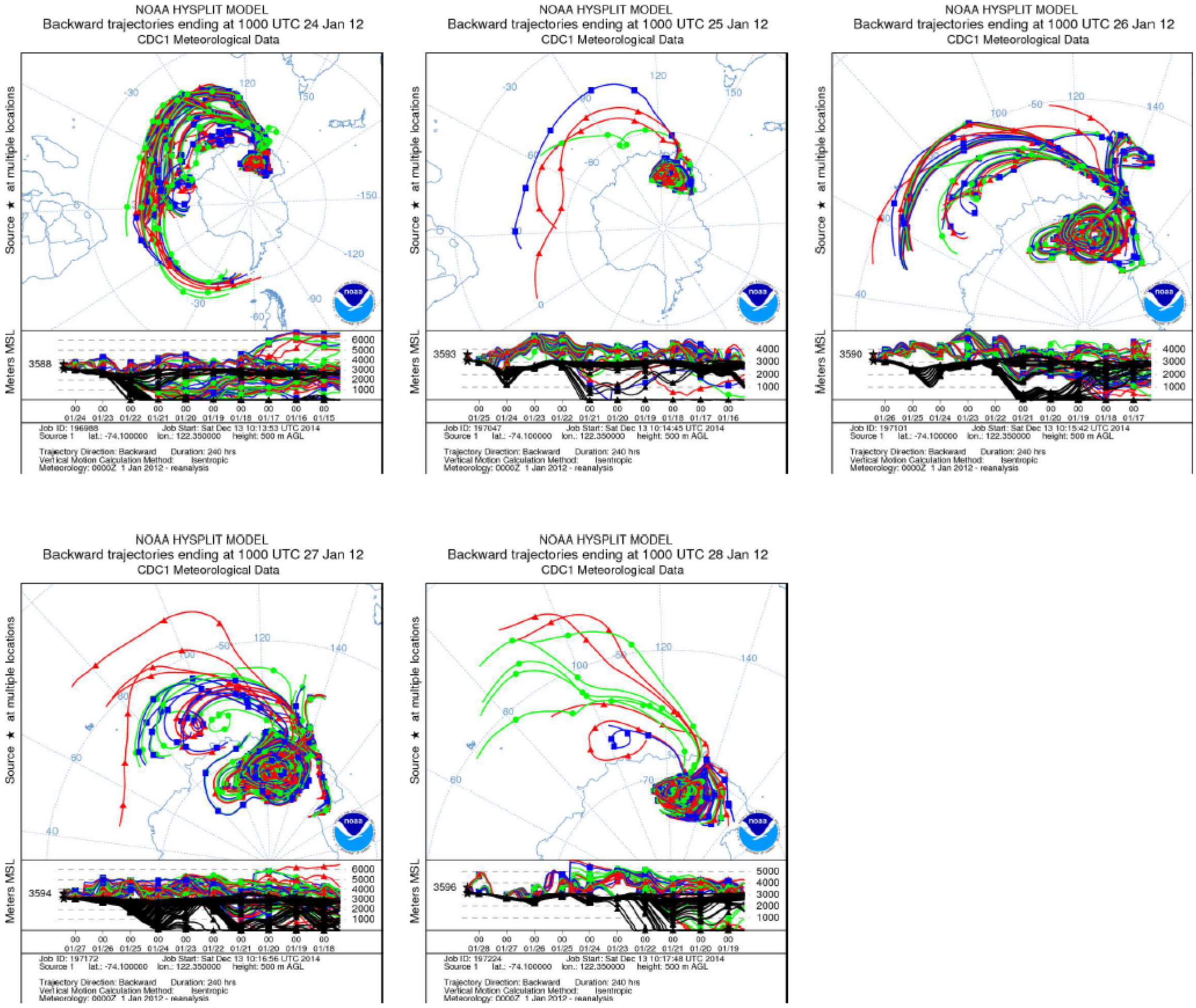

Figure S5. continued

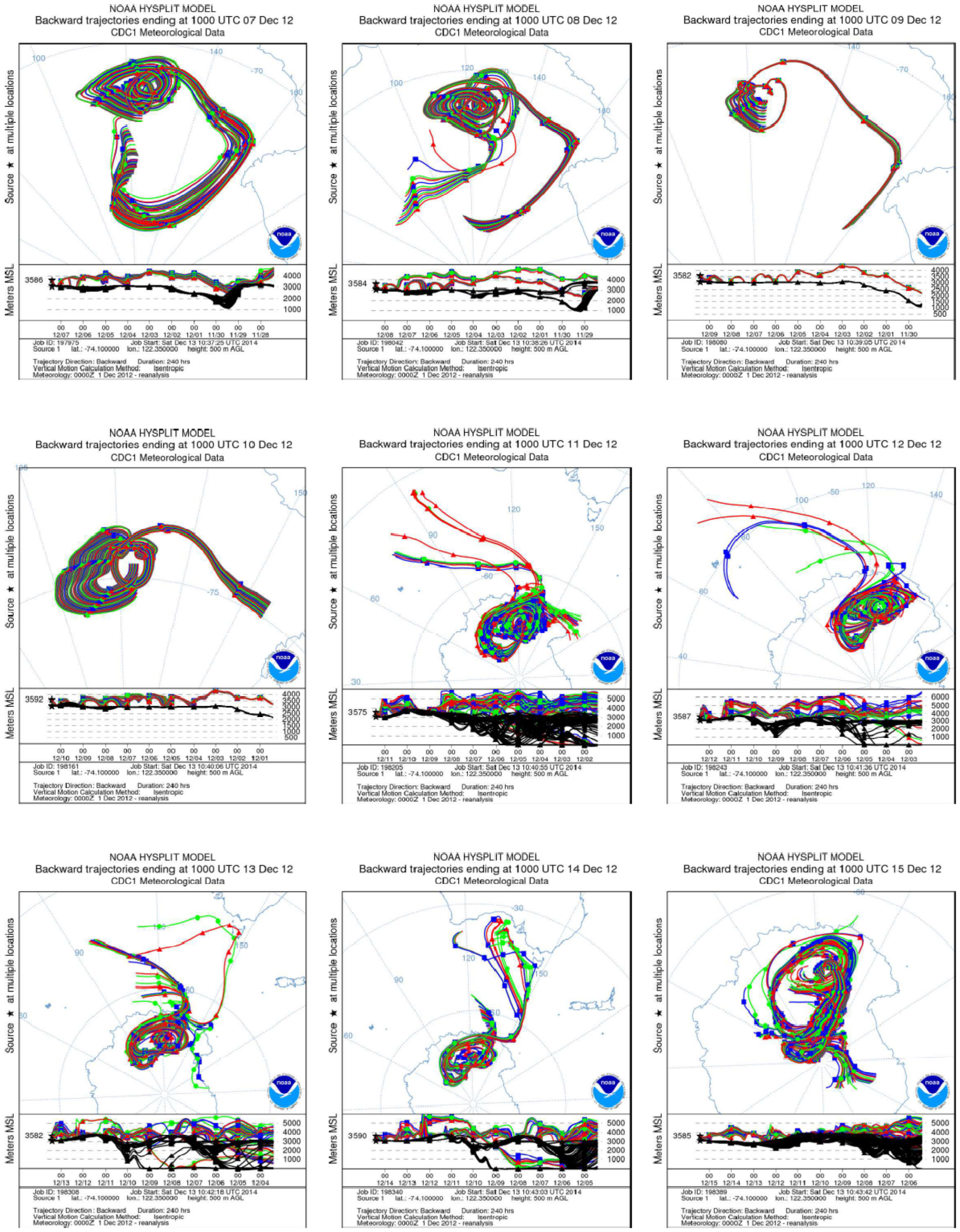

NOAA HYSPLIT MODEL
Backward trajectories ending at 1000 UTC 07 Dec 12
CDC1 Meteorological Data

NOAA HYSPLIT MODEL
Backward trajectories ending at 1000 UTC 08 Dec 12
CDC1 Meteorological Data

NOAA HYSPLIT MODEL
Backward trajectories ending at 1000 UTC 09 Dec 12
CDC1 Meteorological Data

NOAA HYSPLIT MODEL
Backward trajectories ending at 1000 UTC 10 Dec 12
CDC1 Meteorological Data

NOAA HYSPLIT MODEL
Backward trajectories ending at 1000 UTC 11 Dec 12
CDC1 Meteorological Data

NOAA HYSPLIT MODEL
Backward trajectories ending at 1000 UTC 12 Dec 12
CDC1 Meteorological Data

NOAA HYSPLIT MODEL
Backward trajectories ending at 1000 UTC 13 Dec 12
CDC1 Meteorological Data

NOAA HYSPLIT MODEL
Backward trajectories ending at 1000 UTC 14 Dec 12
CDC1 Meteorological Data

NOAA HYSPLIT MODEL
Backward trajectories ending at 1000 UTC 15 Dec 12
CDC1 Meteorological Data

Figure S6. Matrix back-trajectories computed for each 24-h sampling at 500 m agl at the Italian-French base Dome C (DC) from 07th December 2012 to 26th January 2013. Study of the horizontal stability of HYSPLIT model varying the source position of one degree of latitude and longitude from the real coordinates of source.

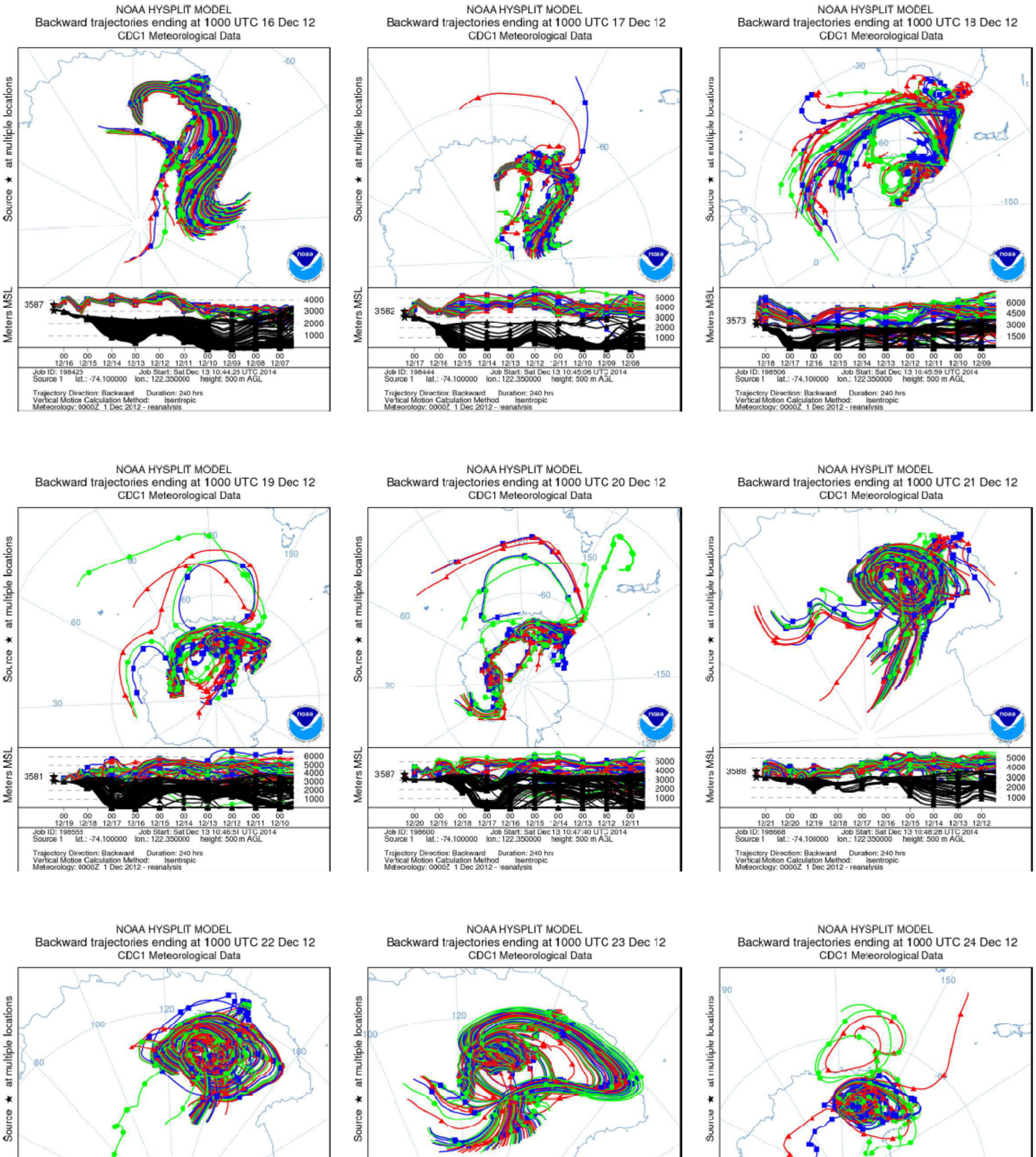

Figure S6. continued

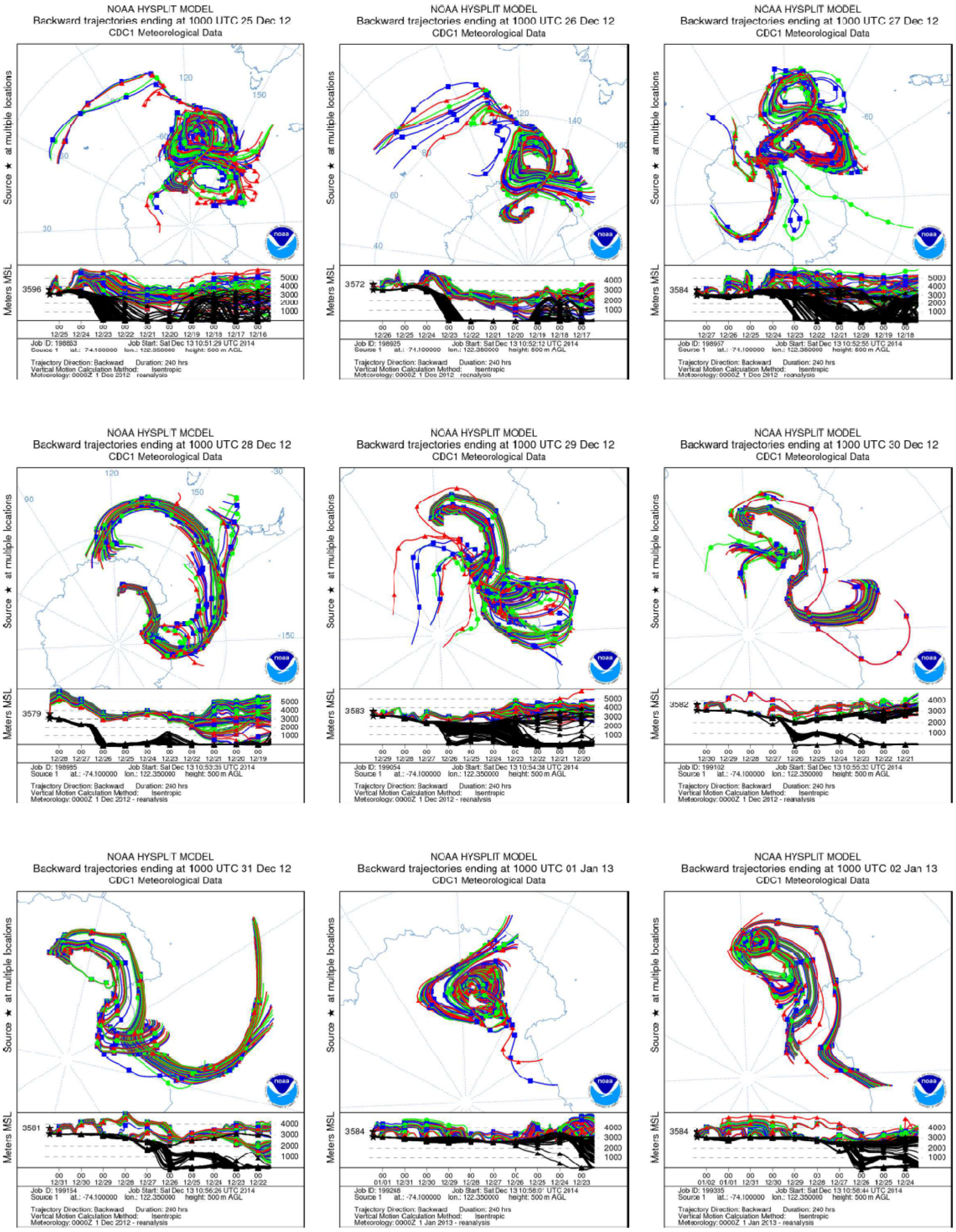
NOAA HYSPLIT MODEL
Backward trajectories ending at 1000 UTC 25 Dec 12
CDC1 Meteorological Data

NOAA HYSPLIT MODEL
Backward trajectories ending at 1000 UTC 26 Dec 12
CDC1 Meteorological Data

NOAA HYSPLIT MODEL
Backward trajectories ending at 1000 UTC 27 Dec 12
CDC1 Meteorological Data

NOAA HYSPLIT MODEL
Backward trajectories ending at 1000 UTC 28 Dec 12
CDC1 Meteorological Data

NOAA HYSPLIT MODEL
Backward trajectories ending at 1000 UTC 29 Dec 12
CDC1 Meteorological Data

NOAA HYSPLIT MODEL
Backward trajectories ending at 1000 UTC 30 Dec 12
CDC1 Meteorological Data

NOAA HYSPLIT MODEL
Backward trajectories ending at 1000 UTC 31 Dec 12
CDC1 Meteorological Data

NOAA HYSPLIT MODEL
Backward trajectories ending at 1000 UTC 01 Jan 13
CDC1 Meteorological Data

NOAA HYSPLIT MODEL
Backward trajectories ending at 1000 UTC 02 Jan 13
CDC1 Meteorological Data

Figure S6. continued

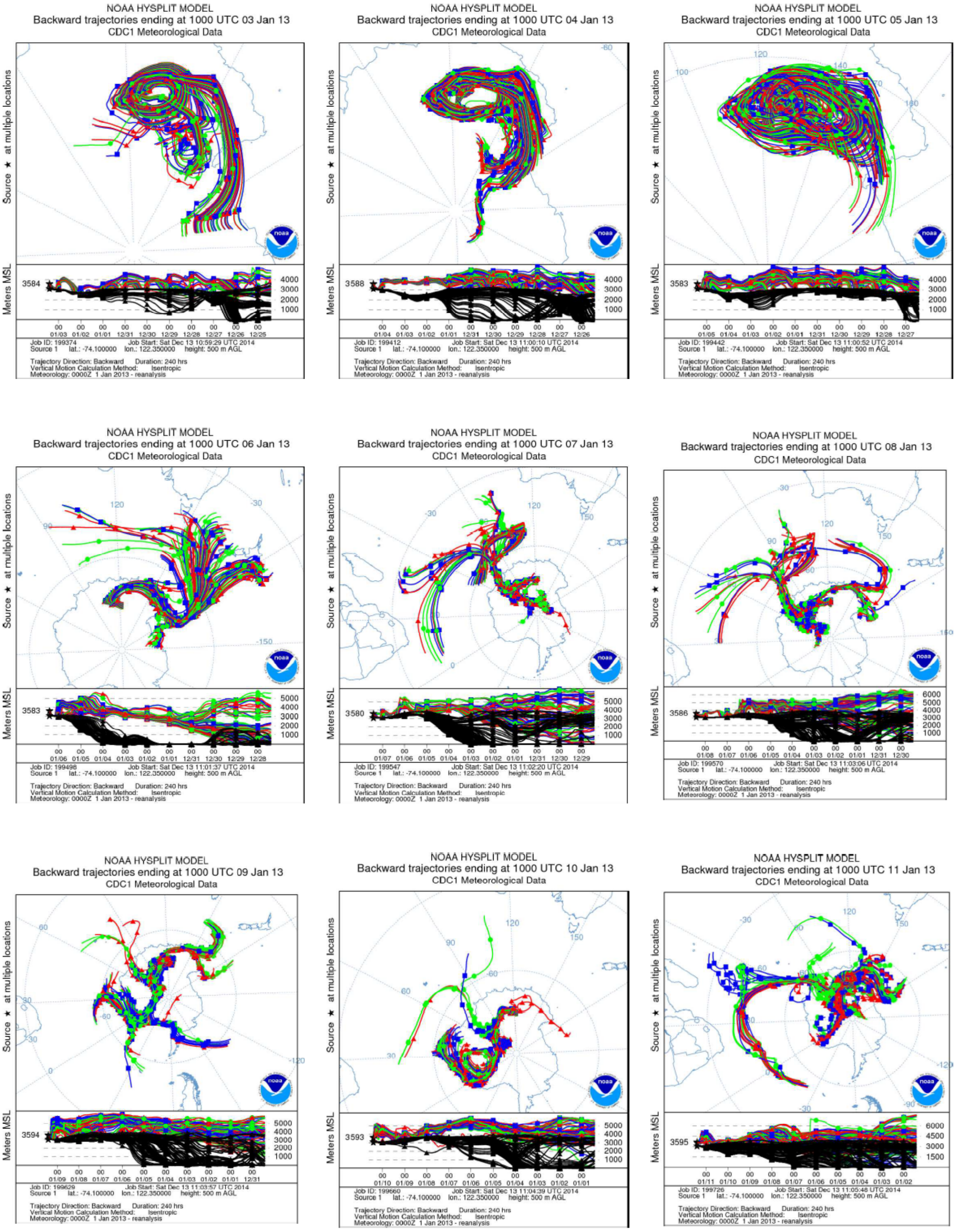

Figure S6. continued

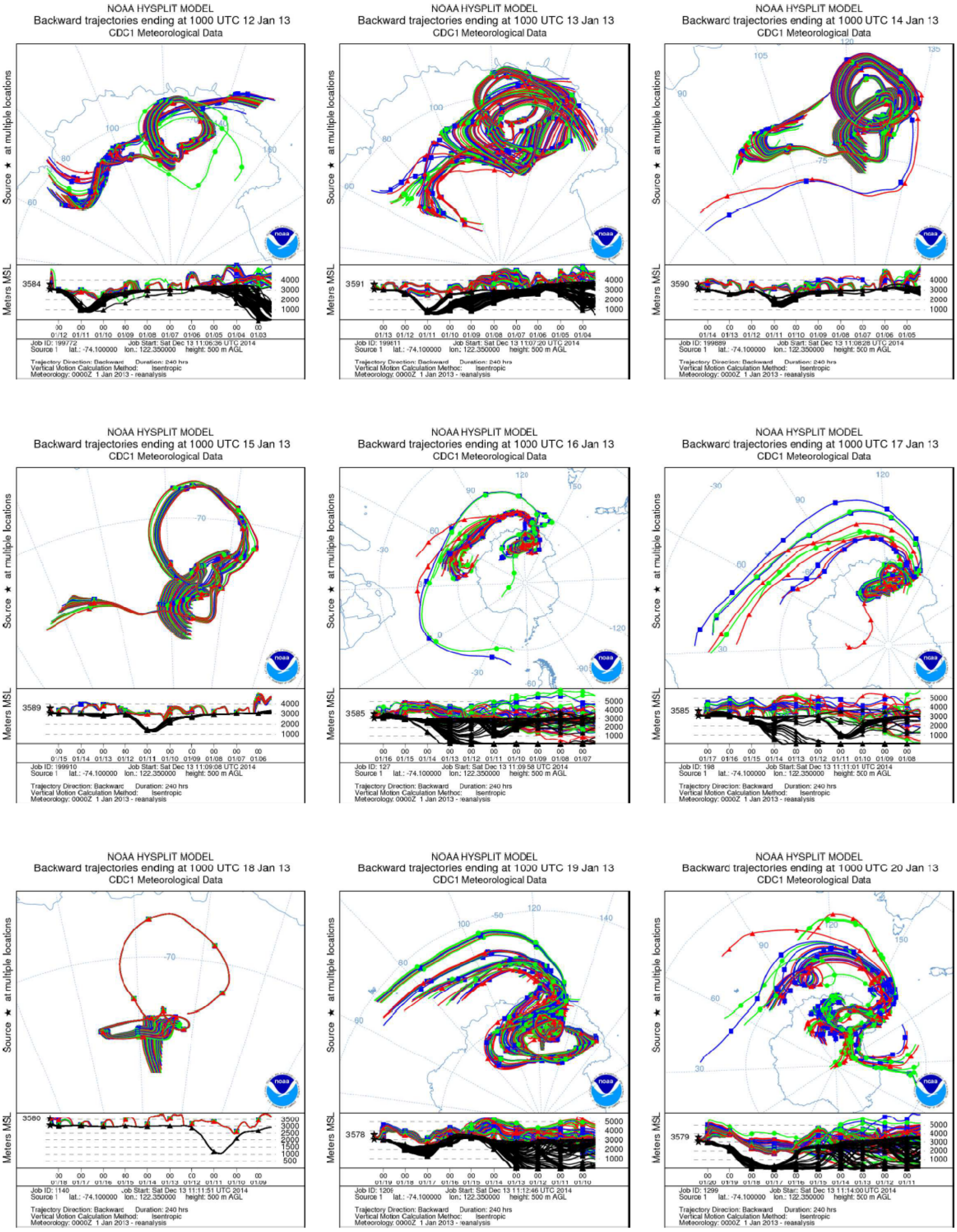

Figure S6. continued

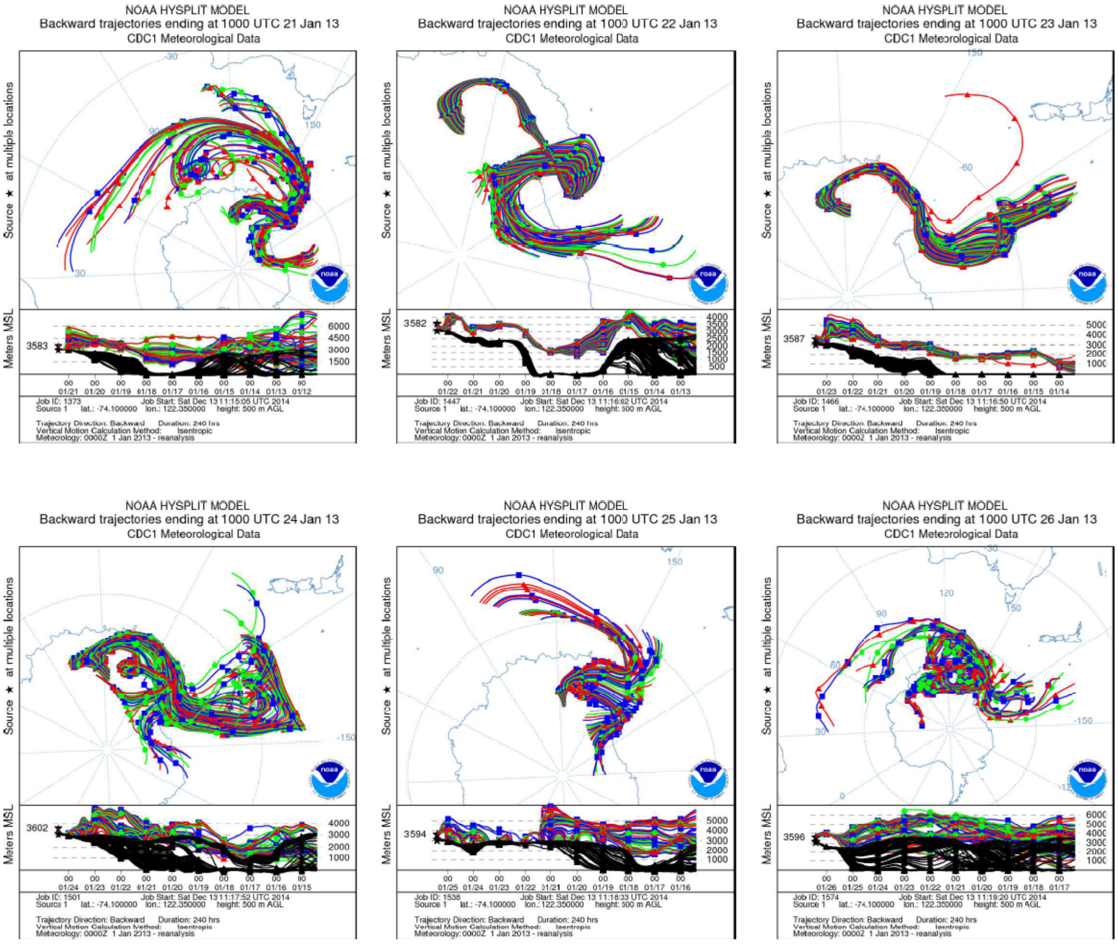

NOAA HYSPLIT MODEL
Backward trajectories ending at 1000 UTC 21 Jan 13
CDC1 Meteorological Data

NOAA HYSPLIT MODEL
Backward trajectories ending at 1000 UTC 22 Jan 13
CDC1 Meteorological Data

NOAA HYSPLIT MODEL
Backward trajectories ending at 1000 UTC 23 Jan 13
CDC1 Meteorological Data

NOAA HYSPLIT MODEL
Backward trajectories ending at 1000 UTC 24 Jan 13
CDC1 Meteorological Data

NOAA HYSPLIT MODEL
Backward trajectories ending at 1000 UTC 25 Jan 13
CDC1 Meteorological Data

NOAA HYSPLIT MODEL
Backward trajectories ending at 1000 UTC 26 Jan 13
CDC1 Meteorological Data

Figure S6. continued

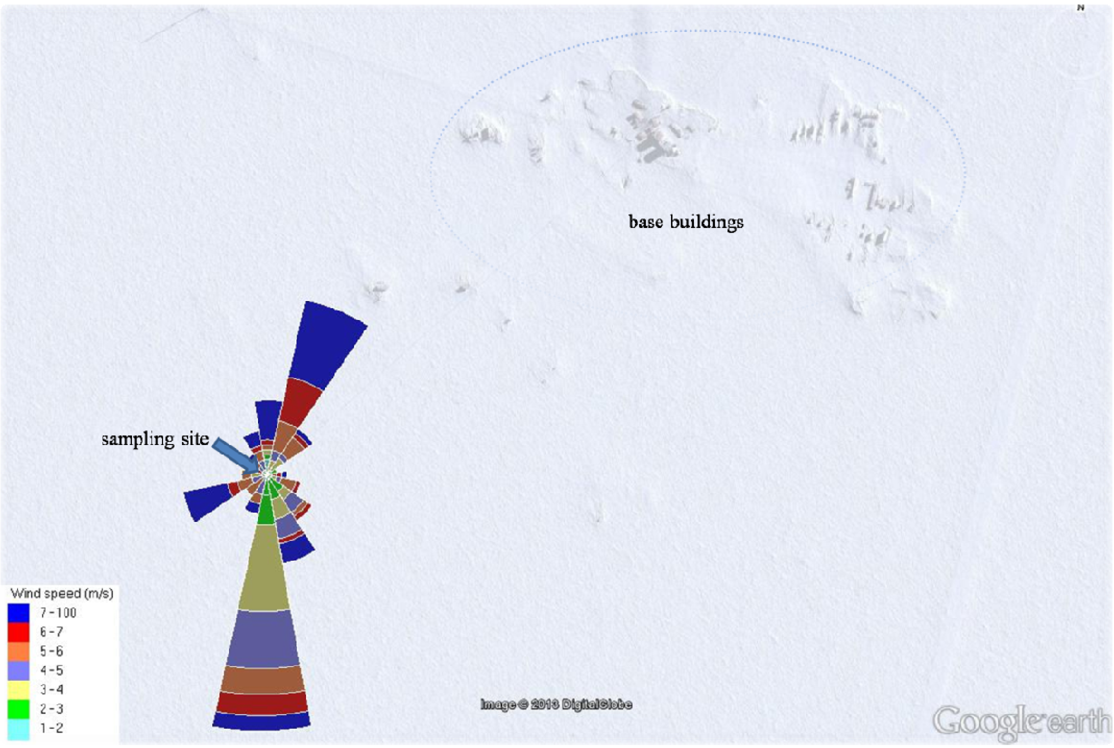

Figure S7. Wind rose of the sample collected from 27 December to 06 January at the Italian-French base “Concordia Station” (Dome C) during the summer in Antarctica 2012-13.

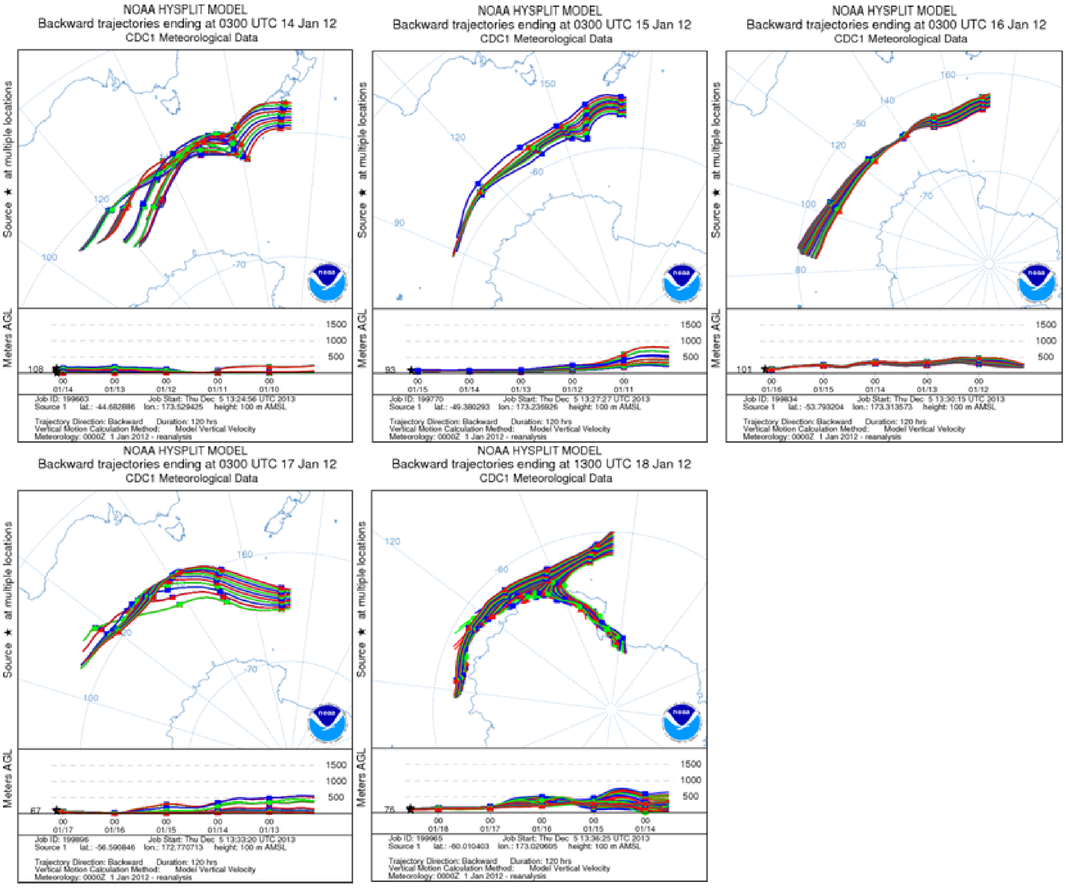

Figure S8A. 5-day back-trajectories of the first sample (from 13 to 18 January) collected during the oceanographic cruise on the R/V Italica during the summer of 2011-12 on the Southern Ocean. The trajectories were computed for each 24-h sampling using a vertical velocity model at 100 m above sea level.

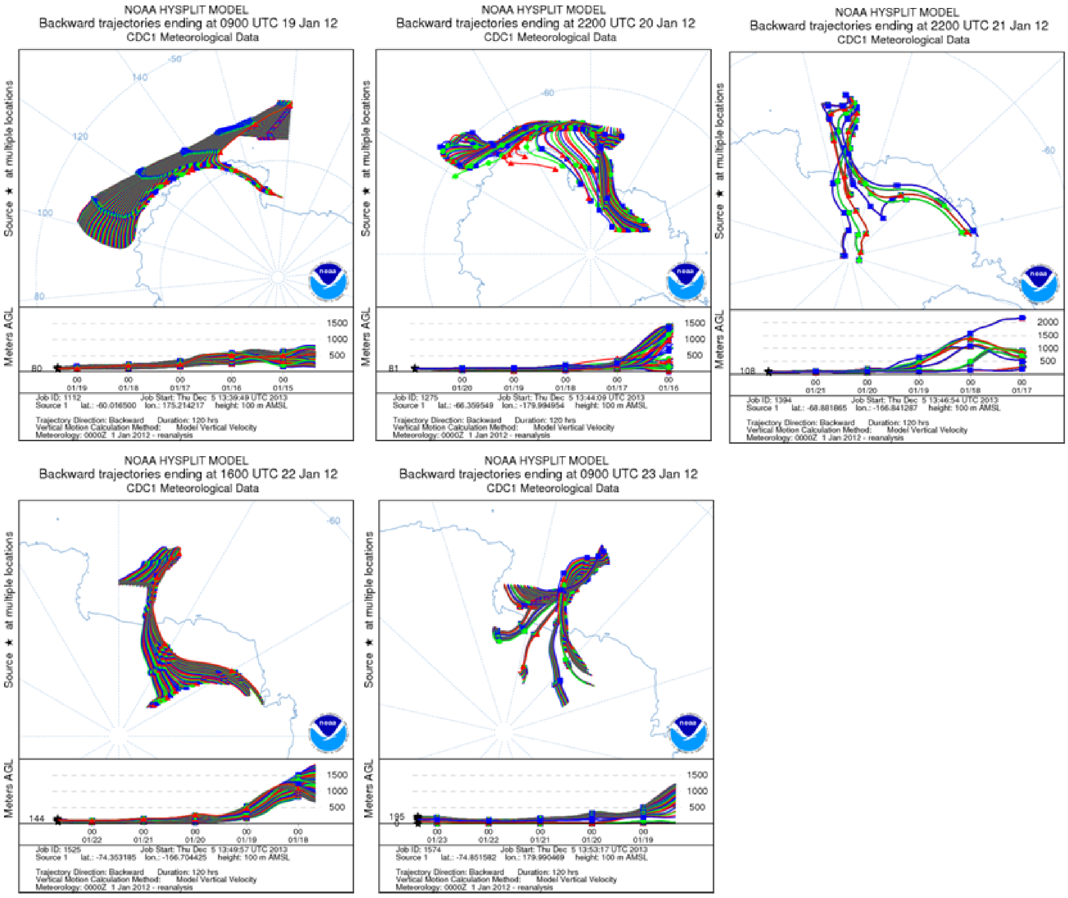

Figure S8B. 5-day back-trajectories of the second sample (from 18 to 23 January) collected during the oceanographic cruise on the R/V Italica during the summer of 2011-12 on the Southern Ocean. The trajectories were computed for each 24-h sampling using a vertical velocity model at 100 m above sea level.

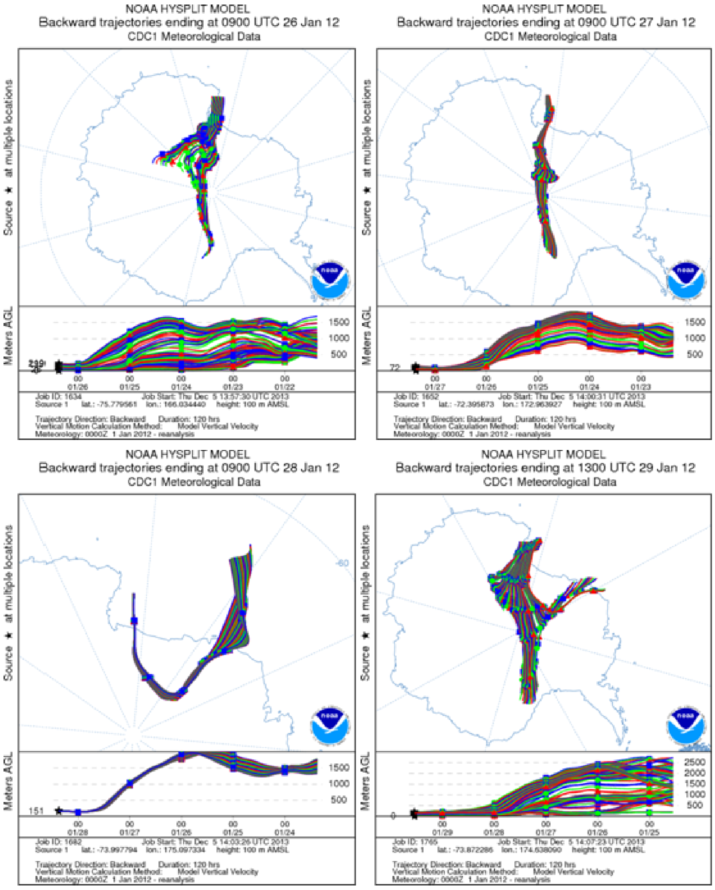

Figure S8C. 5-day back-trajectories of the third sample (from 25 to 29 January) collected during the oceanographic cruise on the R/V Italica during the summer of 2011-12 on the Southern Ocean.. The trajectories were computed for each 24-h sampling using a vertical velocity model at 100 m above sea level.

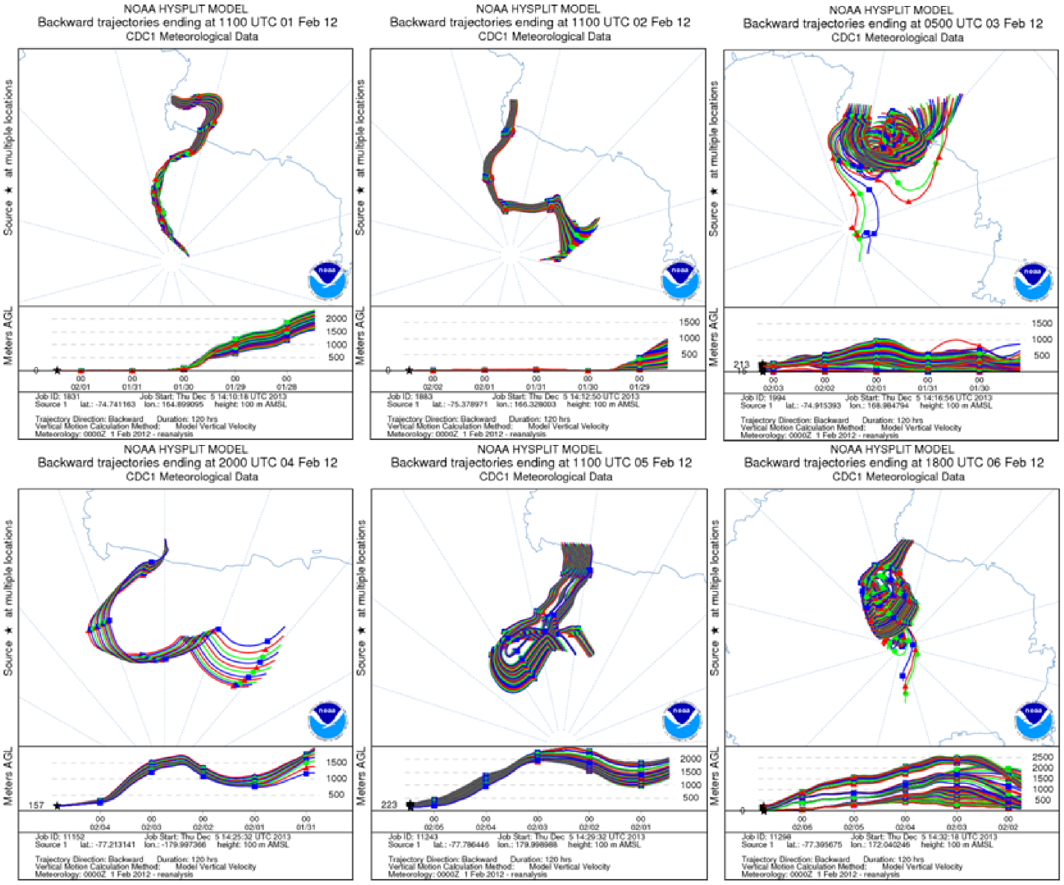

Figure S8D. 5-day back-trajectories of the fourth sample (from 31 January to 6 February) collected during the oceanographic cruise on the R/V Italica during the summer of 2011-12 on the Southern Ocean. The trajectories were computed for each 24-h sampling using a vertical velocity model at 100 m above sea level.

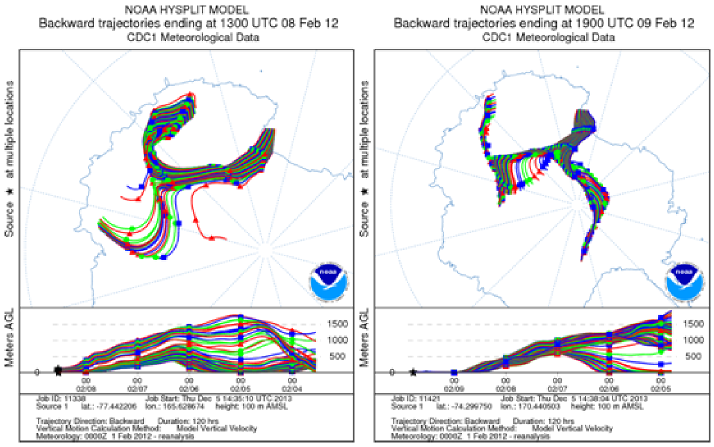
NOAA HYSPLIT MODEL
Backward trajectories ending at 1300 UTC 08 Feb 12
CDC1 Meteorological Data

NOAA HYSPLIT MODEL
Backward trajectories ending at 1900 UTC 09 Feb 12
CDC1 Meteorological Data

Figure S8E. 5-day back-trajectories of the fifth sample (from 7 to 9 February) collected during the oceanographic cruise on the R/V Italica during the summer of 2011-12 on the Southern Ocean. The trajectories were computed for each 24-h sampling using a vertical velocity model at 100 m above sea level.

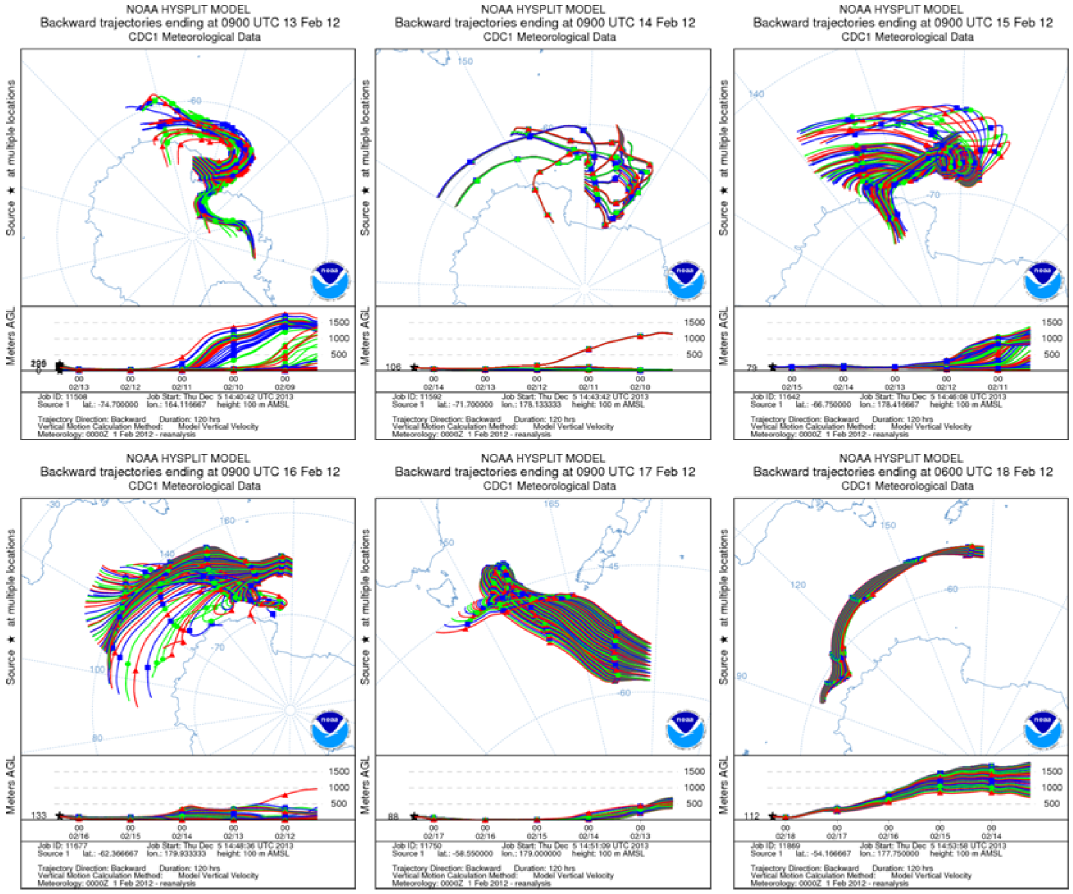
NOAA HYSPLIT MODEL
Backward trajectories ending at 0900 UTC 13 Feb 12
CDC1 Meteorological Data

NOAA HYSPLIT MODEL
Backward trajectories ending at 0900 UTC 14 Feb 12
CDC1 Meteorological Data

NOAA HYSPLIT MODEL
Backward trajectories ending at 0900 UTC 15 Feb 12
CDC1 Meteorological Data

NOAA HYSPLIT MODEL
Backward trajectories ending at 0900 UTC 16 Feb 12
CDC1 Meteorological Data

NOAA HYSPLIT MODEL
Backward trajectories ending at 0900 UTC 17 Feb 12
CDC1 Meteorological Data

NOAA HYSPLIT MODEL
Backward trajectories ending at 0600 UTC 18 Feb 12
CDC1 Meteorological Data

Figure S8F. 5-day back-trajectories of the sixth sample (from 13 to 18 February) collected during the oceanographic cruise on the R/V Italica during the summer of 2011-12 on the Southern Ocean.. The trajectories were computed for each 24-h sampling using a vertical velocity model at 100 m above sea level.

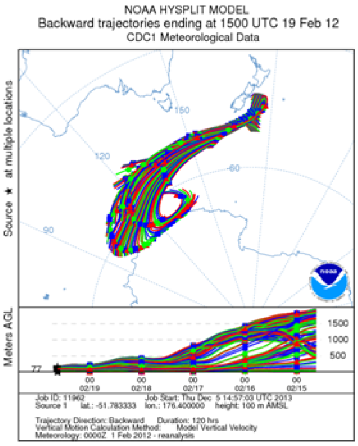

Figure S8G. 5-day back-trajectories of the seventh sample (from 18 to 19 February) collected during the oceanographic cruise on the R/V Italica during the summer of 2011-12 on the Southern Ocean. The trajectories were computed for each 24-h sampling using a vertical velocity model at 100 m above sea level.